Cobalt Oxide Catalysts in the Form of Thin Films Prepared by Magnetron Sputtering on Stainless-Steel Meshes: Performance in Ethanol Oxidation

Květa Jirátová [1,*], Roman Perekrestov [2], Michaela Dvořáková [3], Jana Balabánová [1], Pavel Topka [1], Martin Koštejn [1], Jiří Olejníček [2], Martin Čada [2], Zdeněk Hubička [2] and František Kovanda [3]

[1] Institute of Chemical Process Fundamentals of the CAS, v.v.i., Rozvojová 135, 165 02 Prague, Czech Republic; balabanova@icpf.cas.cz (J.B.); topka@icpf.cas.cz (P.T.); kostejn@icpf.cas.cz (M.K.)

[2] Institute of Physics of the CAS, v.v.i., Na Slovance 2, 182 21 Prague, Czech Republic; perekrestov@fzu.cz (R.P.); olejn@fzu.cz (J.O.); cada@fzu.cz (M.Č.); hubicka@fzu.cz (Z.H.)

[3] Department of Solid State Chemistry, University of Chemistry and Technology, Technická 5, 166 28 Prague, Czech Republic; michaela2.dvorakova@vscht.cz (M.D.); frantisek.kovanda@vscht.cz (F.K.)

* Correspondence: jiratova@icpf.cas.cz; Tel.: +420-220-390-295

check for updates

Abstract: Catalytic total oxidation is an effective procedure to minimize emissions of volatile organic compounds (VOC) emissions in industrial gases. Catalysts in the form of meshes are remarkable as they minimize the internal diffusion of reactants during the reaction as well as the need of expensive active components. In this paper, various conditions of radio frequency magnetron sputtering of cobalt on stainless-steel meshes was applied during catalyst preparation. Properties of the supported Co_3O_4 catalysts were characterized by SEM, XRD, temperature programmed reduction (H_2-TPR), FTIR, XPS, and Raman spectroscopy. Catalytic activity was examined in deep oxidation of ethanol chosen as a model VOC. Performance of the catalysts depended on the amount of Co_3O_4 deposited on the supporting meshes. According to specific activities (the amounts of ethanol converted per unit weight of Co_3O_4), smaller Co_3O_4 particle size led to increased catalytic activity. The catalyst prepared by sputtering in an $Ar+O_2$ atmosphere without calcination showed the highest catalytic activity, which decreased after calcination due to enlargement of Co_3O_4 particles. However, specific activity of this catalyst was more than 20 times higher than that of pelletized commercial Co_3O_4 catalyst used for comparison.

Keywords: coating; thin film; cobalt oxides; meshes; magnetron sputtering; VOC; oxidation

1. Introduction

Catalytic total oxidation is an effective procedure to minimize emissions of volatile organic compounds (VOC) emissions in industrial gases [1,2]. We have demonstrated a high catalytic activity of cobalt oxide catalysts in oxidation of ethanol [3], which is very often emitted from pharmaceutical plants or printing works. High activity of cobalt oxide catalysts was also observed in total oxidation of other organic compounds, like propane [4–6], toluene [5,7], CO [8], or formaldehyde [9]. Formerly we have reported a remarkable oxidation activity of cobalt-containing oxides deposited on anodized aluminum foils [10].

Catalysts intended for fast chemical reactions have to work at short residence times, i.e., at high throughputs of reaction mixture. Under such conditions, pelletized catalysts show high pressure drops, and thus, catalysts bed of high free volume is necessary. Various forms of catalysts are used for this type of reaction: Monoliths, foams, meshes, etc. The well-known application of a metal gauze catalyst is the oxidation of ammonia with air to nitric oxide used in the production of nitric acid and

the hydrogen cyanide synthesis [11]. Moreover, catalysts in the form of meshes were also recently studied in environmental processes such as complete oxidation of volatile organic compounds [12–14] or N_2O decomposition [15].

Stainless-steel materials used as catalyst supports display, compared to ceramic ones, much better stability, which is essential for many industrial applications. They have the advantages of low cost, high mechanical strength, and sufficient thermal conductivity, better than ceramic materials have. On the other hand, their disadvantage is a very smooth surface, which cannot sufficiently strongly fix the active components. To overcome this problem, it is necessary to modify the stainless-steel materials by various techniques to form porous oxide layer on their surface. Del Río et al. [16] prepared mesoporous nanowires of Co_3O_4 on stainless-steel wires by the ammonia evaporation-induced method and used them in steam reforming of ethanol. Thin Co_3O_4 films were deposited on stainless-steel grid mesh using one-step chemical vapor deposition method [17]. Klyushina et al. [15] prepared supported Co_3O_4 catalysts by heating the cobalt hydroxide synthesized electrochemically on stainless-steel meshes. The K/Co_3O_4 stainless-steel wire mesh catalyst combined suitable features of active cobalt species with the effective utilization of all catalytic components active in N_2O decomposition. Ahlstroem-Silverstand et al. [18] applied catalytically active wire meshes to combust different pollutants present in flue gases from biofuel combustion. In their work, alumina was spray-deposited onto wire meshes of Kanthal AF (8–20 Tyler mesh) with a magnetron spray equipment. Magnetron sputtering system with argon and oxygen atmosphere was used to prepare one hundred nanometers thick Co_3O_4 film on Co foil or double-side polished silicon wafers [19].

Recently we have studied the procedure of coatings of meshes with cobalt-containing oxides. We prepared thin layers of Co–Mn oxides by deposition of thin layers of their precursors on meshes made of aluminum [3]. For comparison, we prepared a catalyst by deposition of a $Co(OH)_2$ slurry on aluminum meshes and used it for abatement of volatile organic compounds, namely ethanol. Though the structured catalysts had nearly 50 times lower content of active components, they showed approximately the same activity as the pelletized catalyst from commercial Co_3O_4. Unfortunately, the layers were not sufficiently adhered to the substrate. Later, we replaced aluminum meshes for stainless-steel ones, as the stainless-steel meshes are stronger than aluminum meshes after anodization or chemical treatment, applied before their coating by metal oxides precursors [20]. The plasma-enhanced physical vapor deposition (PVD) using radio frequency (RF) magnetron sputtering and high-power impulse magnetron sputtering (HiPIMS) in $Ar+O_2$ atmosphere was applied for coating the meshes covered by Co_3O_4 thin films (about 300 nm in thickness). On the so prepared meshes, cobalt hydroxide precursors were deposited by cathodic reduction in cobalt nitrate-containing aqueous solution; the precursors were then transformed to Co_3O_4 by heating at 500 °C in air. Rather poor adhesion of the cobalt oxide layer prepared by electrochemical deposition was significantly improved, when the catalysts were coated with additional Co_3O_4 thin film by magnetron sputtering. The catalysts prepared using RF magnetron sputtering were more active than analogous catalysts prepared using the HiPIMS process. Perekrestov et al. [21] confirmed similar observation.

In the present study, conditions of cobalt oxides deposition on stainless-steel wire meshes by RF magnetron sputtering were examined in more detail. The RF magnetron sputtering of metallic cobalt under inert and oxidation atmosphere either followed or not by calcination in air, as well as time of sputtering was studied and the effect of preparation conditions on the performance of resulting catalysts in the total oxidation of organic compound, namely ethanol, was investigated. Properties of the catalysts prepared under examined conditions were compared with those of the catalysts prepared by conventional impregnation of the stainless-steel meshes with cobalt nitrate aqueous solution followed by subsequent calcination and by pelletizing of commercial Co_3O_4 catalyst.

2. Results

The following cobalt oxide catalysts were prepared on stainless-steel meshes: Three catalysts (labeled as Co-RF-x, where x = 1; 2; 3) differing in Co_3O_4 layer thickness were prepared by RF

magnetron sputtering of Co in 90% N_2 and 10% H_2 forming gas, two catalysts (labeled as Co-RF-ox/ap and Co-RF-ox) were prepared by RF magnetron sputtering of Co in an oxidation $Ar+O_2$ atmosphere, and a catalyst prepared by conventional impregnation of meshes (Co-I) was included for comparison. Properties of all supported catalysts were compared with those of the particles prepared by pelletizing of commercial Co_3O_4 (labeled as PEL). The catalysts were characterized by chemical analysis, SEM, XRD, Kr physisorption, temperature programmed reduction (H_2-TPR), Raman spectroscopy, FTIR, and XPS. Catalytic activity of the samples was evaluated in deep oxidation of ethanol.

2.1. Characterization of the Catalysts

Content of cobalt oxides in the supported catalysts was determined as the difference between the weight of the samples after calcination and the weight of the stainless-steel meshes used as supports for deposition of active components and related to the total sample weight. The content of cobalt oxides in the catalysts prepared by magnetron sputtering varied from 0.73 to 1.44 wt.% (Table 1).

Table 1. Characteristic data of the catalysts examined by XRD, FTIR, and temperature programmed reduction (TPR).

Sample	Co_3O_4 Content/%	Weight [a] Loss/%	D [b] (Co_3O_4)/nm	FT-IR $/\nu_{Co-O}$ (cm^{-1})	TPR [c]/ mmol $H_2 \cdot gCoOx^{-1}$	TPR T_{max}/°C
Co-RF-1	0.73	8	33.7	694; 649; 613; 555; 505	15.1	378
Co-RF-2	0.79	12	32.5	694; 649; 613; 555; 505	15.2	360
Co-RF-3	1.44	31	37.9	694; 655; 630; 613; 548	14.4	381
Co-RF-ox/ap	0.93	3	7.1	688; 653; 605; 547	14.0	266 [d]; 358
Co-RF-ox	0.75	3	21.9	688; 605; 547	14.7	367
Co-I	1.10	60	31.7	670; 547	14.6	262 [d]; 358; 554
PEL	97.0	-	75.3	660; 547	15.6	426

[a] Weight loss observed after adhesion test related to the weight of deposited oxides. [b] Calculated as mean coherent domain length in [311] direction using Scherrer's formula. [c] (25–900 °C). [d] Shoulder.

Surface areas of the stainless-steel-supported cobalt oxide catalysts were low, as it turned out by krypton physisorption at −196 °C; the S_{BET} values of 0.0038 and 0.0042 m^2 g^{-1} were found for the Co-RF-1 and Co-RF-3 samples, respectively. Surface area of the sample prepared by pelletizing of the commercial Co_3O_4 was also low (2.2 m^2 g^{-1}) but more than 500 times higher than those found for the samples prepared on the stainless-steel meshes.

Surface morphology of cobalt oxide layers deposited on stainless-steel meshes is demonstrated in Figure S1 in Supplementary. SEM images of the samples prepared by RF magnetron sputtering of cobalt in an inert argon atmosphere followed by heating in air showed rather compact and homogeneous coatings with small pores; very likely, the formed coatings consist of the interconnected oxidized cobalt particles resembling foams (Figure S1a–c). Increasing amount of cobalt oxides on the meshes due to prolonged magnetron sputtering procedure resulted in deposition of thicker layers but their structure remained identical. The Co-RF-ox/ap sample prepared by RF magnetron sputtering of cobalt in oxidation $Ar+O_2$ atmosphere showed quite different morphology of the arising cobalt oxide particles as isolated platelets of cobalt oxides can be seen on the surface (Figure S1d). After calcination of this sample at 500 °C in air, the morphology was changed and globular aggregates of very fine crystals of cobalt oxide can be seen in the SEM image of the Co-RF-ox catalyst (Figure S1e). SEM image of the Co-I catalyst prepared by impregnation of stainless-steel meshes with cobalt nitrate aqueous solution and subsequent heating at 500 °C in air showed relatively non-homogeneous coating of the wires surface with clusters of globular cobalt oxide particles (Figure S1f) and, therefore, higher tendency of the coating to peeling can be expected.

Adhesion of deposited cobalt oxide to the stainless-steel support was evaluated by a simple test, when the catalysts were immersed in an ultrasonic bath at room temperature and treated for 10 min in acetone; the weight loss was then determined after drying the samples and related to initial weight of the deposited cobalt oxides (Table 1). The catalysts prepared by magnetron sputtering

showed very good adhesion to the support as they exhibited only low weight loss of several percent; the lowest value was found for the Co-RF-ox/ap sample (2.9% related to weight of deposited cobalt oxide). Adhesion of the coatings decreased with increasing content of cobalt oxide in the catalysts. Larger crystals observed in the SEM images indicated higher tendency to be removed from the surface in comparison with the smaller ones. Both catalysts prepared by cobalt sputtering in the oxidation Ar+O_2 atmosphere (the Co-RF-ox/ap and Co-RF-ox catalysts) showed the highest adhesion while the Co-I catalyst prepared by impregnation the lowest one; weight loss of 60% of the deposited oxide was found for this sample.

Powder X-ray diffraction is important technique for the investigation of bulk structure, which is very important, as many of the catalyst characteristics depend on it. Results of the XRD measurements are shown in Figure 1. The diffraction peaks were ascribed to Co_3O_4 (PDF 04-006-3982); no peaks corresponding to CoO or metallic Co were observed. It indicated practically complete oxidation of the cobalt coatings obtained by magnetron sputtering in inert argon atmosphere after subsequent heating in air, as well as direct oxidation of sputtered cobalt particles in Ar+O_2 atmosphere. The distinct sharp diffraction peaks at approximately 51 and 60° 2θ corresponded to a Fe0.65Cr0.1Ni0.25 phase (PDF 04-019-2390). They were ascribed to the stainless-steel support. Full width in half maximum (FWHM) values were evaluated from the measured powder XRD patterns and mean coherence lengths of Co_3O_4 in [311] direction were calculated (Table 1) using Scherrer's formula D = k λ/(β cosθ), where λ is the X-ray wavelength, β is the full width at half maximum (FWHM) of the diffraction peak corresponding to (311) plane of Co_3O_4, θ is the corresponding diffraction angle, and k is a constant (k = 0.9 was used in calculation). The smallest D value of 7.8 nm was found for the Co-RF-ox/ap sample prepared by magnetron sputtering of cobalt in Ar+O_2 atmosphere. The mean coherence length increased to 23.5 nm after heating of this sample at 500 °C in air and thus, better structure ordering of the Co-RF-ox catalyst could be expected. The catalysts prepared by magnetron sputtering of cobalt in the inert argon atmosphere followed by heating in air showed very similar powder XRD patterns and only small differences in mean coherence lengths ranging from 32.5 to 38 nm. The largest D value of 75 nm was determined for the pelletized commercial Co_3O_4. SEM images of the pellets interior (Figure S1g) also revealed aggregates of cobalt oxide particles with considerably larger size in comparison with those observed in the examined supported catalysts. Powder XRD pattern of the pelletized commercial Co_3O_4 catalyst is shown in Figure 1 as well. This catalyst contained, apart from Co_3O_4, small amount of CoO (PDF 04-013-5837) admixture. Graphite (PDF 04-016-6288) was also detected, as it was added as a lubricant during pelletizing of the cobalt oxide.

Raman spectroscopy is a non-destructive technique providing detailed information about chemical structure, phase and polymorphy, crystallinity, and molecular interactions. Raman spectra of the examined catalysts are presented in Figure 2. Raman spectra of the catalysts prepared by magnetron sputtering showed five bands at 194, 484, 528, 620, and 692 cm^{-1}. As found by Hadjiev et al. [22] and Zhang et al. [23], five Raman-active modes and bands were identified at 194 (phonon mode F2g), 482 (Eg), 522 (F2g), 618 (F2g), and 691 (A1g) cm^{-1} modes of cubic-phase Co_3O_4. Similarly, Tang et al. [24] found analogous bands at 482, 519, 621, and 690 cm^{-1} in the Raman spectrum of Co_3O_4. The following Raman bands were reported for CoO: 672 and 468 cm^{-1} [22] and 675 and 455 cm^{-1} [24]. There is not a big difference between the spectra of Co-RF-2 and Co-RF-3 samples, but both differ to some extent from the spectrum of Co-RF-1 catalyst, which shows peaks slightly shifted to lower wavenumbers. With respect to the low concentration of cobalt oxides in the Co-RF-1 catalyst, the reason for the shift could be tighter bonds between the cobalt oxides and the support. Bands' intensities in the Raman spectrum of this catalyst are lower than those of the Co-RF-2 and Co-RF-3 catalysts are. Intensity of the bands was increasing with increasing Co_3O_4 content. The low band intensity and broadening in the spectrum of Co-RF-1 sample could indicate smaller particles of cobalt oxide but SEM images of the Co-RF-x samples (Figure S1a–c) did not show different morphology of the Co_3O_4 coatings and D values obtained from powder XRD data indicated very similar structure ordering of the deposited

Co_3O_4. The bands of CoO were not found in the Raman spectra of the samples as more intensive and well-apparent bands of Co_3O_4 could overlap them.
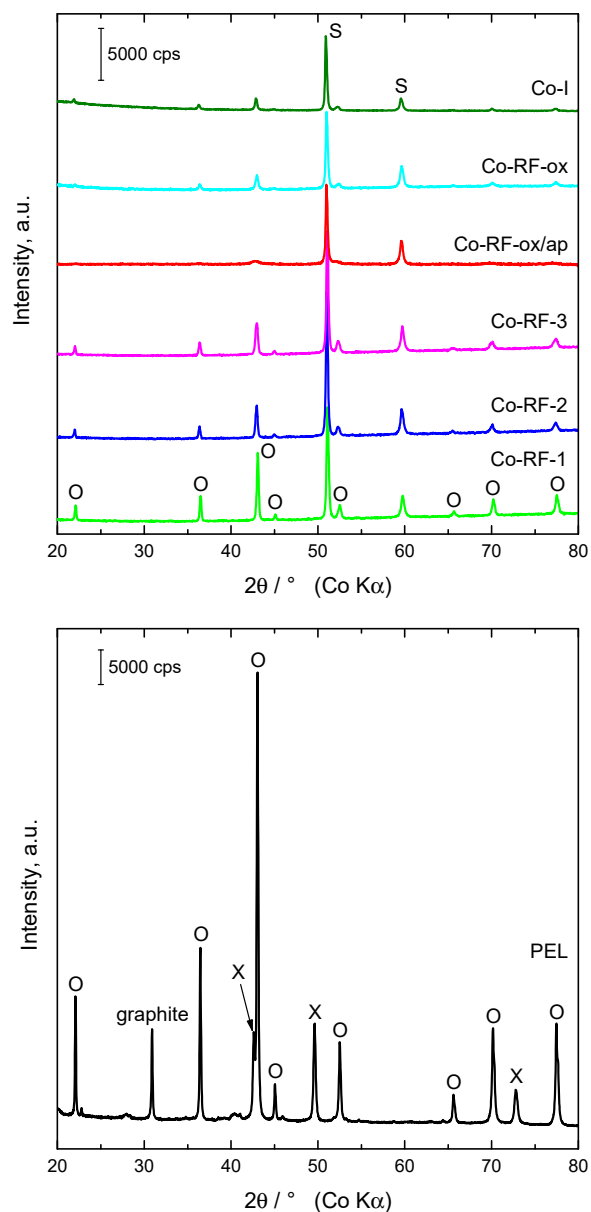

Figure 1. Powder XRD patterns of the cobalt oxide catalysts prepared over meshes and the pelletized commercial Co_3O_4 (the PEL sample below). O—Co_3O_4, S—stainless-steel support, X—CoO.

Fourier transform infrared spectroscopy (FTIR) is a valuable non-destructive characterization technique used to identify various oxides including cobalt oxides. The FTIR spectrum of CoO is characterized by a transverse optical (TO) phonon below 400 cm^{-1} and by a higher frequency longitudinal optical (LO) phonon at 580 cm^{-1} [25]. Tang et al. [24] and Bao et al. [19] observed a broad infrared band around 510 cm^{-1}. Variation in the values of the band positions are likely caused by different experimental arrangement used in the mentioned reports; nevertheless, the band at about 510 cm^{-1} can be used for identification of CoO. In the FTIR spectra of Co_3O_4 thin film samples, positions of four phonons were observed at 673 (LO), 654 (TO), 592 (LO), and 554 (TO) cm^{-1}. The LO/TO ratios depended on particle size and the incident angle of FTIR beam intensity [19]. In the transmission mode, Lenglet et al. [25] reported very near values at 694 (LO), 655 (TO), 607 (LO), and 543 (TO) cm^{-1} of the bands in the infrared spectrum of the Co_3O_4 spinel.
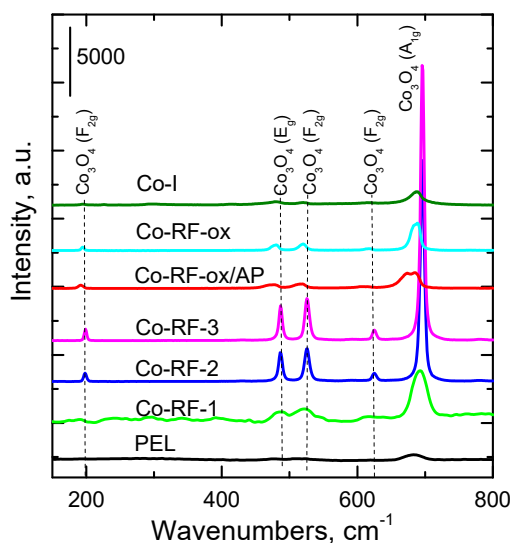
Figure 2. Raman spectra of the examined supported cobalt oxide catalysts.

In our study, FTIR spectra were recorded for the cobalt oxide coatings prepared by magnetron sputtering on stainless-steel meshes, the coating obtained by calcination of the mesh impregnated with cobalt nitrate aqueous solution and for the pelletized Co_3O_4 (Figure 3). The bands at 694, 649, 613, 547, and 505 cm^{-1} were observed in the spectrum of Co-RF-1 sample with the lowest Co_3O_4 content, obtained by magnetron sputtering in inert atmosphere and subsequent heating in air. In accord with report of Bao et al. [19], the bands at 694 and 613 cm^{-1} can be ascribed to Co_3O_4 (LO) and those at 649 and 555 cm^{-1} to Co_3O_4 (TO) bands. The band at 505 cm^{-1} could be assigned to CoO. In the sample with higher cobalt oxide content (Co-RF-3), the intensity of the bands at 510 and 649 cm^{-1} were slightly decreasing and a new band at 630 cm^{-1} appeared. Very likely, non-stoichiometric Co_3O_4 was partly originating during preparation of thicker cobalt oxide coatings [26].
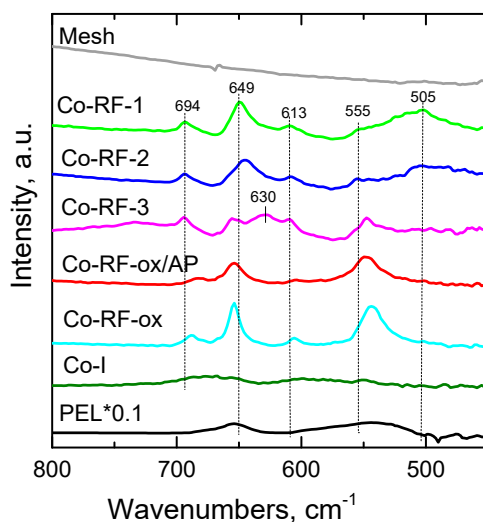

Figure 3. FTIR spectra of the examined cobalt oxides catalysts.

The as-prepared Co-RF-ox/ap sample obtained by magnetron sputtering in oxidation atmosphere showed bands of lower intensity than those previously mentioned. The reason for the observation can be smaller size of particles and a poor structure ordering indicated by powder XRD measurements. The positions of the two main bands (555 and 660 cm^{-1}) remained identical as those in the samples prepared by sputtering in inert atmosphere and only the position of the 694 cm^{-1} band was shifted to lower wavenumbers (688 cm^{-1}). After heating the Co-RF-ox/ap sample in air, the positions of the bands

in the obtained Co-RF-ox catalyst did not change but their intensities became more pronounced due to improved structure ordering. The Co-I catalyst and pelletized commercial Co_3O_4 exhibited two very broad bands with maxima at 656 and 544 cm^{-1}, which originated, very likely, from superimposition of other bands due to high cobalt oxide contents in these catalyst.

Temperature programmed reduction (H_2-TPR) is a widely used tool for the characterization of metal oxides, mixed metal oxides, and metal oxides dispersed on a support. The TPR method yields quantitative information of the reducibility of the oxides surface, as well as the heterogeneity of the reducible surface. The TPR profiles of all prepared catalysts are shown in Figure 4. According to former reports [27,28], reduction of Co_3O_4 proceeds in two steps: Co_3O_4 is reduced to CoO above 300 °C and CoO is subsequently reduced to cobalt at about 400 °C. Arnoldy et al. [29] observed the reduction of Co_3O_4 in one peak around 330 °C, and the peaks corresponding to partial reduction were almost indistinguishable. All our examined samples were reduced in one narrow peak with prevailing temperature maximum around 375 °C. The samples were completely reduced before reaching the temperature 500 °C and it means that all cobalt oxide can be utilized in ethanol oxidation [30]. A shoulder at about 400 °C indicates presence of a cobalt compound of lower reducibility, very likely CoO [23]. In our TPR experiments, T_{max} temperatures of the supported catalysts varied from 310 to 381 °C, while that one of the pelletized Co_3O_4 was 426 °C. Nearly identical course of TPR was observed for all Co-RF-x samples and the commercial Co_3O_4 catalyst. Reduction of the Co-RF-ox/ap sample proceeded at substantially lower temperatures (310 °C) showing small peaks at 275 and 184 °C. After calcination of this sample, the small peaks appearing at low temperatures disappeared.
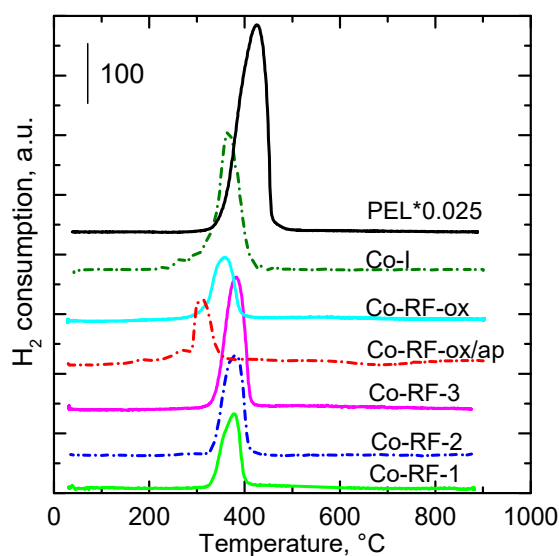
Figure 4. H_2-TPR profiles of the supported cobalt oxide catalysts and pelletized commercial Co_3O_4 catalyst (PEL).

The finding indicates that small particles are present in the Co-RF-ox/ap sample, which were converted to larger particles upon calcination and were reduced at 367 °C. The Co-I catalyst exhibited similar course of reduction as the Co-RF-ox; this can be explained by similar particle sizes and structure ordering of cobalt oxide particles in these two catalysts (Figure S1e–f, Table 1).

Amounts of hydrogen consumed during H_2-TPR experiments in the temperature range from 25 to 900 °C and calculated per gram of cobalt oxides deposited on the meshes are summarized in Table 1. If the cobalt ions in cobalt oxide were only Co^{3+} or only Co^{2+} and reduced to Co^0, the H_2 consumption would be 16.6 or 13.3 mmol g^{-1}, respectively. In case of reduction of Co_3O_4, theoretical consumption of hydrogen for its reduction to metal would be 15.48 mmol H_2 g^{-1}. As revealed in the H_2-TPR results, the H_2 consumptions for Co oxides reduction were 15.6, 15.1, and 15.2 mmol H_2 g^{-1}

for the PEL, Co-RF-1, and Co-RF-2 catalysts, respectively, and from 14.7 to 14.0 mmol H_2 g^{-1} for the remaining catalysts.

Surface analysis of the fresh and used (i.e., after the catalytic testing) Co-RF-ox/ap and Co-RF-ox catalysts was performed using XPS. Metals from the stainless-steel supports (Fe, Cr, Ni, and Mo) were not detected in the spectra, which points to the fact that the meshes were completely covered with cobalt oxides. A carbon tape used for the fixing of the meshes to the holder manifested itself in high concentration of C and O (Table 2). As the samples used in the XPS measurements were in the form of stainless-steel meshes covered by cobalt oxides, charging of the samples could not be fully compensated by a carbon correction, which would be influenced by underlying carbon tape. Thus, it was necessary to calibrate the spectra according to oxygen (corresponding to binding energy of the metal-oxygen bond in metal oxide at 529.5 eV).

**Table 2.** Surface composition of selected catalysts determined by XPS (at.%).

Sample		Co	O	C
Co-RF-ox/ap	Fresh	7.2	28.2	64.6
Co-RF-ox/ap	Used	7.8	29.7	62.4
Co-RF-ox	Fresh	3.2	24.2	72.6
Co-RF-ox	Used	4.2	21.2	74.6

Cobalt surface concentrations in the fresh and used catalysts were practically the same (Table 2). However, we found a difference between these values of the Co-RF-ox/ap and Co-RF-ox samples, as surface concentration of Co of the Co-RF-ox/ap was higher than that of Co-RF-ox sample. As the dimensions of the samples applied during XPS measurements were identical, the difference in surface concentrations of Co cannot be explained by variation of the parameter. The phenomenon can be elucidated by larger surface area or lower amount of carbon impurities adsorbed on the catalysts surface due to higher catalytic activity of the Co-RF-ox/ap samples. Surfaces of both samples were covered exclusively with Co_3O_4 (Table 3). The finding is documented by deconvolution of the Co 2p3/2 spectra to CoO and Co_3O_4 contributions according to Biesinger [31]. The fresh Co-RF-ox sample contains a low additional amount of Co^{2+} as follows from deconvoluted XPS spectrum (Figure 5).

Table 3. Concentrations of cobalt species and O (in at.%) from XPS spectra of the examined catalysts.

Sample	O 1s				Co 2p3/2		O(529.5):Co
BE, eV	529.5	531.1–531.5	531.9–532.5	532.7–533.5	780.0	780.5	
Co-RF-ox/ap							
Fresh	12.9	7.0	5.6	2.7	7.2	0	1.80
Used	14.4	6.5	5.4	3.5	7.9	0	1.83
Co-RF-ox							
Fresh	6.0	6.9	7.9	3.4	3.2	0.04	1.85
Used	8.8	5.3	5.1	2.1	4.2	0	2.07

Deconvolution of oxygen spectrum of the Co-RF-ox/ap sample revealed several peaks (Table 3). The peak at 529.5 eV can be assigned to metal oxide (lattice oxygen, O^{2-}), the peak at 531.3 eV can be ascribed to low-coordinated or the adsorbed oxygen bonded to cobalt as O^-. The next line with maximum at 532.3 eV can be ascribed to adsorbed OH^- species as well as to simple bond of oxygen to carbon. Bonds of oxygen to carbon can arise as bonds to carbon tape and other adventitious carbon contamination. The fourth peak observed at 533.1 eV can be assigned to adsorbed water. The deconvoluted O 1s spectra indicated that both the Co-RF-ox/ap and Co-RF-ox sample after catalytic tests contained more lattice oxygen than the fresh samples.
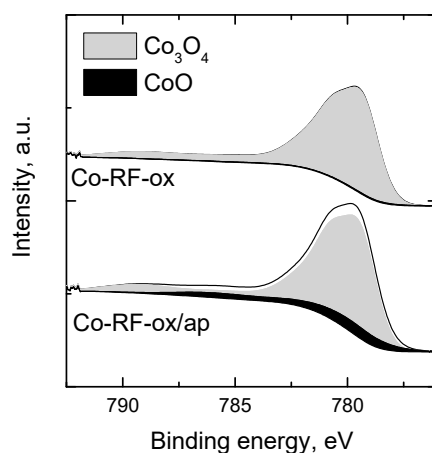
Figure 5. Deconvolution of Co $2p_{3/2}$ XPS spectra of the Co-RF-ox/ap and Co-RF-ox catalysts to CoO and Co_3O_4 contributions (their parameters are taken from Biesinger [31]).

The composition determined by XPS shows a higher O:Co ratio than 1.3 corresponding to Co_3O_4. The origin of this discrepancy is not easy to elucidate. It can be caused either by non-homogeneity or by different surface morphology of the sample, which could alter response factors used for calculation of composition. Either way, the O:Co ratio is similar for all samples except Co-RF-ox/ap. The increase of amount of oxygen bound to cobalt in the Co-RF-ox/ap can be partially explained by higher presence of Co^{2+} (additional CoO) in the fresh sample.

2.2. Catalytic Activity and Selectivity

Deep oxidation of ethanol was used as a model catalytic reaction to examine catalytic activity and selectivity of the catalysts. Performance of the catalysts was characterized in the terms of T_{50} temperature, i.e., temperature, at which 50% ethanol conversion was observed.

Ethanol conversions in dependence on reaction temperature are shown in Figure 6.
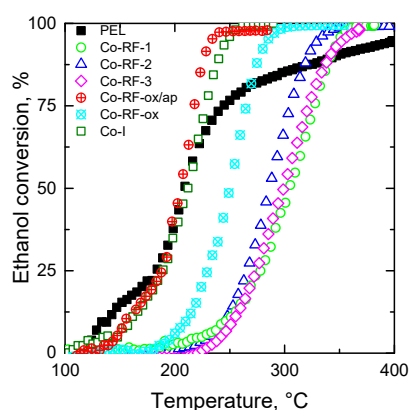
Figure 6. Dependence of ethanol conversion over the catalysts on reaction temperature. Reaction conditions: 760 ± 10 ppm of ethanol in air, temperature ramp 2 °C min^{-1}, F/W = 21 ± 1 L h^{-1} g^{-1}.

The curves exhibited an S-shape typical of light-off measurements. The reaction temperatures necessary for 50% ethanol conversion (T_{50}) varied in the range from 210 to 291 °C (Table 4). For the Co-RF-x catalysts, the T_{50} value increased with decreasing amount of the cobalt oxides deposited on the meshes. Among the catalysts prepared by magnetron sputtering, the lowest T_{50} temperature (205 °C) was found for the non-calcined Co-RF-ox/ap catalyst. The PEL catalyst exhibited the lowest T_{50} temperature in the set of examined catalysts. However, it can be seen from Figure 6 that a substantially

higher temperature was necessary to apply to meet complete ethanol conversion to CO_2 with this catalyst in contrast to all other catalysts.

Table 4. Physical-chemical and catalytic properties of the examined catalysts (reaction conditions: Space velocity F/W = 21 ± 1 L h g^{-1}, 760 ± 10 ppm of ethanol in air, temperature ramp 2 °C min^{-1}).

Sample	Co_3O_4 Content/ wt.%	T_{50}/ °C	T_{95CO2}/ °C	AcA [a]/ppm/°C	CO [b]/ppm/°C	X_{200}/%	r_{200}/ $mmol_{EtOH}$ g_{Co3O4}^{-1} h^{-1}
Co-RF-1	0.73	291	364	500/325	110/356	2.1	2.1
Co-RF-2	0.79	287	356	511/314	94/350	1.6	1.2
Co-RF-3	1.44	285	351	512/314	78/357	3.2	1.6
Co-RF-ox/ap	0.93	216	244	433/223	12/234	43.0	32.4
Co-RF-ox	0.75	250	311	542/275	68/296	6.0	5.4
Co-I	1.10	212	265	454/240	62/255	36.6	22.1
PEL	97.0	210	399 [c]	195/199	0/-	39.4	0.29

[a] Maximum concentration of acetaldehyde in the reaction mixture and corresponding reaction temperature.
[b] Maximum concentration of carbon monoxide in the reaction mixture and corresponding reaction temperature.
[c] 93% conversion of organic compounds.

In case of oxidation catalysts, selectivity is often more important parameter than the T_{50} temperature as the by-products formed during the reaction may be more detrimental for human health and environment than the original organic compound. The typical course of reaction components obtained during increasing reaction temperature at ethanol oxidation can be seen in Figure 7. The $T_{95}CO_2$ (temperature necessary for 95% conversion of all organic compounds to CO_2) was therefore employed to assess the selectivity of the catalysts. Taking into account the objective of the catalytic reaction, i.e., the complete abatement of volatile organic compound, the $T_{95}CO_2$ temperatures (Table 4) also reveal the order of efficiency of the catalysts. According to this parameter, the Co-RF-ox/ap sample is more efficient than the Co-I catalyst, followed by the Co-RF-ox catalyst. The Co-RF-x catalysts exhibited lower efficiency than their above-mentioned analogues. Finally, the PEL catalyst showed the lowest efficiency of all catalysts as it attained only 93% conversion to CO_2 at 399 °C.
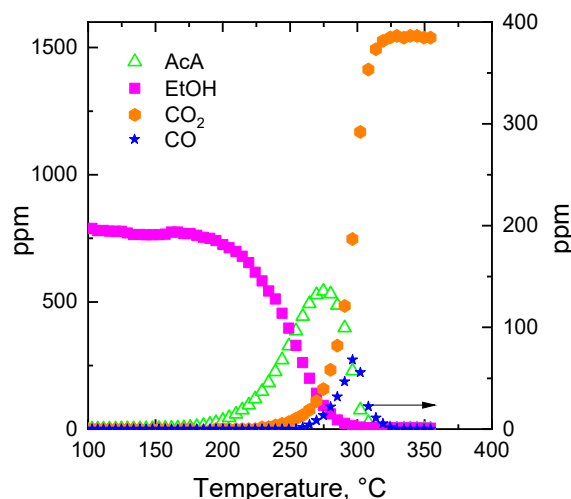
Figure 7. Concentrations of ethanol, acetaldehyde (AcA), CO, and CO_2 in dependence on reaction temperature obtained during ethanol oxidation over the Co-RF-ox/ap catalyst.

As the amounts of active components in the catalysts slightly differed, the specific reaction rates at 200 °C were calculated to compare the activity of the catalysts (Table 4). Performance of the Co_3O_4 species in the examined catalysts showed that the RF-x catalysts do not differ too much from each other. On the other hand, the RF-Co-ox/ap catalyst prepared by reactive magnetron sputtering in Ar+O_2 mixture exhibited twenty times higher activity. After its calcination, the activity of resulting RF-Co-ox catalyst decreased six times, very likely due to increase in structure ordering of cobalt oxide particles

(Table 1). The activity of the Co-I catalyst prepared by impregnation of the meshes with cobalt nitrate solution and heating was the highest. However, with respect to the practical application, deposited cobalt oxide layer was not sufficiently adhered to the support (Table 1).

The highest specific activity among all examined catalysts was observed with the Co-RF-ox/ap sample (32.4 mmol EtOH g_{oxides}^{-1} h^{-1}), while the lowest one was determined for the pelletized Co_3O_4 catalyst (PEL sample, 0.3 mmol EtOH g_{oxides}^{-1} h^{-1}). The concentrations of by-products formed during the reaction were similar for all examined catalysts (Table 4); the lowest formation of CO was achieved with the most active Co-RF-ox/ap catalyst.

3. Discussion

Experimental results carried out in this study demonstrated that the cobalt oxide catalysts prepared by magnetron sputtering exhibit very good adhesion of the Co_3O_4 layer to the support. They exhibited only low weight loss during treatment in an ultrasonic bath, which was used as a simple test to evaluate the adhesion of deposited oxide; the lowest value was found for the catalyst prepared by Co sputtering in oxidation $Ar+O_2$ atmosphere (2.9% related to weight of deposited cobalt oxide). Adhesion of the coatings slightly decreased with increasing cobalt oxide content in the catalysts. The oxide coatings consisting of larger crystals observed in the SEM images (Supplementary Figure S1) indicated higher tendency to fall away from the mesh surface in comparison with those consisting of the smaller crystals.

All supported catalysts contain cobalt oxide with average valence of Co corresponding to Co_3O_4, whose presence in the catalysts was confirmed by powder XRD, Raman, and FTIR spectroscopy. As mentioned in the Results, consumptions of hydrogen for Co oxides reduction in the examined catalysts were 15.1, 15.2, and 15.6 mmol H_2 g^{-1} for the Co-RF-1, Co-RF-2, and PEL catalysts, respectively, and from 14.7 to 14.0 mmol H_2 g^{-1} for the remaining ones. As theoretical consumption of H_2 for reduction of Co_3O_4 is 15.5 mmol H_2 g^{-1}, the H_2 consumptions found during TPR experiments, lower than theoretical one, indicate that small amounts of CoO in the supported catalysts cannot be excluded. The presence of CoO was confirmed in the Co-RF-1 sample (Figure 3) as the band with maximum at 505 cm^{-1} (assigned to CoO) was found in its FTIR spectrum. XRD did not have to record the presence of CoO due to its low concentration in the active phase or too small particles. Similar H_2 consumption during TPR experiments to the theoretical one was observed with the pelletized commercial Co_3O_4, despite the fact that CoO admixture was confirmed by powder XRD in this sample. Therefore, precisely differentiating the CoO and Co_3O_4 contents in the cobalt oxide coatings prepared on the stainless-steel meshes from the H_2-TPR measurements was not possible, but, in spite of this, formation of non-stoichiometric Co_3O_4-type oxides with lower Co valence than corresponding to Co_3O_4 can be expected in the catalysts prepared by magnetron sputtering.

The highest catalytic activity (lowest T_{50} temperature) among the catalysts prepared by magnetron sputtering was found for the non-calcined Co-RF-ox/ap catalyst prepared by Co sputtering in oxidation atmosphere. This catalyst showed the worst structure ordering of Co_3O_4 (mean coherence length D of 7.1 nm) among all catalysts (Table 1). After calcination at 500 °C, performance of the catalyst decreased (T_{50} was 250 °C) as the result of better structure ordering (D = 21.9 nm) and changes in the morphology of the Co_3O_4 coatings (see Figure S1d,e in Supplementary). Slightly higher catalytic performance was observed with the Co-I catalyst prepared by impregnation (T_{50} = 212 °C). However, the weight loss of the Co oxides in the adhesion test of this catalyst was 60% (Table 1), whereas the catalysts prepared by magnetron sputtering exhibited much better adhesion of the active phase: The weight loss was ranging from 3% to 31% in dependence on amount of the deposited Co oxides in the catalysts and the method of their preparation. The highest specific activity of the Co-RF-ox/ap corresponds well with the morphology and size of the cobalt oxide particles: The cobalt oxide coating prepared by reactive magnetron sputtering in $Ar+O_2$ atmosphere consisted of relatively large, well-developed platelet crystals with diameter of about 200 nm, while the PEL catalyst exhibited nearly 10 times larger particles (Figure S1). In the presence of this catalyst, no CO was formed. The finding could be caused

by the effect of internal diffusion in the pellets, which results in prolonged contact time of reaction components with the active centers.

Based on the catalysts' characteristics, high activity in oxidation of ethanol of the catalysts prepared by magnetron sputtering can be attributed to the excellent redox properties of Co_3O_4, the amount of lattice oxygen, and structure morphology. The high catalytic activity can be mainly attributed to low-temperature reducibility caused by the surface oxygen species, bulk oxygen mobility, and active oxygen vacancies [6,32]. Cations in high oxidation states function as oxidizing species while the oxygen species inserted into the oxidation product come from surface oxide ions, i.e., nucleophilic lattice oxygen. According to Finocchio [33], the activity of the p-type semiconducting oxides such as Co_3O_4 is ascribed to "excess" nucleophilic oxygen species (O^{2-}) at the surface, associated with the presence of trivalent cobalt (Co^{3+}). Therefore, the deep oxidation of ethanol over Co_3O_4 thin film can proceed with Mars–van Krevelen type mechanism. This is confirmed by the fact that the temperature range, in which Co_3O_4 particles of thin films are reduced (230–410 °C), corresponds well with the temperature range within which ethanol conversion is observed.

4. Materials and Methods

4.1. Catalysts Preparation

Conditions of catalyst preparation by RF magnetron sputtering are described in detail in [21]. Stainless-steel meshes (composition 71 wt.% Fe, 11 wt.% Ni, 16 wt.% Cr, and 2 wt.% Mo, mesh size 0.40 mm, wire of 0.22 mm in diameter) in the form of circle with outer diameter of 25 mm were used as supports. The meshes were cleaned mechanically before metal deposition using a brush with detergent, then washed in distilled water, and degreased in acetone for 10 min in an ultrasonic bath. Then, the meshes were dried at room temperature in air.

The cobalt deposition by RF magnetron sputtering was performed in a Veeco vacuum chamber evacuated to a base pressure of $2 \cdot 10^{-3}$ Pa. The magnetron of Kurt J. Lesker Torus 2HV equipped with the high strength magnets was used as a sputtering gun. The planar magnetron was connected to the Advanced Energy ATX 600 RF power supply. Before the cobalt deposition, the standard ion scrubbing process was used for the stainless-steel meshes pretreatment to improve adhesion of the deposited thin films. The chamber was filled with the forming gas (90% N_2, 10% H_2) at the pressure of 20 Pa. The RF discharge was then ignited for 300 s to clean and activate the stainless-steel surface. A holder of six meshes (electrically connected) was placed at axial distance of 70 mm from the target face; this distance ensured homogeneity of film thickness better than 5% for all the meshes placed on the holder. In order to cover both sides of the meshes, the deposition process (except ion scrubbing) was repeated. The cobalt thin films were sputtered in pure argon atmosphere (Ar mass flow rate of 15 sccm) from the cobalt target (99.95% Co, Kurt J. Lesker) of 50 mm in diameter. The working pressure was adjusted by a gate valve throttling the turbomolecular pump to 1 Pa. The RF power delivered into the discharge was set on 200 W. The cobalt films with various thickness (approximately 0.5, 0.75, and 1.0 μm) were prepared after deposition times 10, 15, and 20 min. Then, the samples were calcined for 8 h at 500 °C in air. After calcination, the thickness of the layers increased to about 1.2, 1.8, and 2.4 μm, respectively. The prepared catalysts were denoted as Co-RF-x, where x is equal to 1, 2, or 3 denoting increasing amount of the cobalt layer deposited on the mesh (Table 1).

Analogous procedure was applied for reactive RF magnetron sputtering of cobalt oxide films. The target was reactively sputtered in Ar+O_2 atmosphere to yield cobalt oxide thin films. The films were sputtered from the cobalt target at power of 200 W under pressure of 2.5 Pa in a mixture of argon and oxygen at the Ar and O_2 flow rates of 80 and 5 sccm, respectively. The cobalt oxide films of about 2 μm in thickness were obtained after 75 min deposition. The as-appeared (ap) sample was labeled as Co-RF-ox/ap. After heating this sample at 500 °C for 4 h in air, a different sample was obtained and labelled as Co-RF-ox.

Conventional impregnation of the stainless-steel meshes with nearly saturated aqueous solution of cobalt nitrate at room temperature was also applied. The impregnation step was repeated three times, with drying and calcination at 500 °C for 4 h in air after each impregnation, to meet cobalt oxide content in the catalyst of about 1.0 wt.%, i.e., the content comparable with that found in the catalysts prepared by magnetron sputtering. This catalyst was labeled as Co-I.

The reference cobalt oxide catalyst in the form of pellets was prepared by pelletizing of commercial Co_3O_4 (OMG Kokkola Chemicals, Oy, Finland) with 3 wt.% of graphite on tablet machine to obtain pellets of dimension 5×3 mm. In order to gain pellets with sufficient mechanical strength, optimum pelletizing pressure was necessary to find. The catalyst was labeled as PEL.

4.2. Catalysts Characterization

Powder X-ray diffraction (XRD) patterns were recorded using a Bruker AXS D8 diffractometer (Germany) with Co Kα radiation ($\lambda = 0.179$ nm) in 2θ range 10–80°, step size 0.02°. The qualitative analysis was performed with a HighScore Plus 4.0 software package (PANanalytical, Almelo, The Netherlands).

Krypton physisorption was performed using an ASAP 2020 Micromeritics instrument (Norcross, GA, U.S.A.) after degassing at 200 °C for 24 h under 1 Pa vacuum [34]. The adsorption–desorption isotherms of krypton at −196 °C were treated by the standard Brunauer–Emmett–Teller (BET) procedure for the p/p^0 range = 0.05–0.25 to calculate the specific surface area S_{BET}. A new vessel made of stainless steel was used for the measurements (Patent application PV 2019–380, Prague, Czech Republic) [35].

The surface morphology of the samples was observed using scanning electron microscope Tescan FERA3 (Brno, Czech Republic). In order to maintain all surface details at high resolution, no conductive layer was applied for coating of the observed samples.

Raman spectra were recorded on DXR Raman Microscope spectrometer (Thermo Scientific, Waltham, MA, U.S.A.) equipped with confocal Olympus microscope and multichannel thermoelectrically cooled CCD detector (Center Valley, PA, U.S.A.). The Nd:YAG laser (wavelength 532 nm, maximum power 10 mW) (Thermo Scientific, Waltham, MA, U.S.A.) was used as excitation source. Measurement conditions were 1–3 mW laser power, 100 accumulations of 30 s scans, grating with 900 lines mm^{-1}, and aperture 25 μm pinhole. Magnification 50x provided measurement spot-size ~1 μm^2. To ensure an average spectrum, several spectra from each sample were averaged out.

FTIR spectrometer Avatar 360 (Nicolet, Madison, Wisconsin, U.S.A.) was used to measure infrared spectra of samples between 360 and 4000 cm^{-1} (resolution 1.93 cm^{-1}, 300 scans, 1 s per scan). In order to obtain spectra from the catalysts deposited on stainless-steel meshes, specular reflection mode was used for the measurements and clear stainless-steel mesh as a background. To obtain the spectrum of pelletized Co_3O_4, common ATR mode was applied. Before measurement, the pellets were crushed, and the powder was pressed against the ZnSe crystal.

XPS spectra were measured with two samples, Co-RF-ox/ap and Co-RF-ox. Samples were placed on a holder by a carbon tape. Superficial elemental analyses were performed by X-ray Photoelectron Spectrometer Kratos ESCA 3400 (base pressure lower than $5 \cdot 10^{-7}$ Pa), using non-monochromatic Mg X-ray source (Mg Kα, 1253.4 eV). As the samples were placed on a carbon tape, a carbon correction was not possible to use and for that reason, all spectra were corrected to a metal bound oxygen (529.5 eV). Shirley background was subtracted and elemental compositions of the layers were calculated from the corresponding areas. Composition under the surface layer was not possible to determine, as cobalt easily reduces by Ar$^+$ ions during the etching.

Temperature programmed reduction (H$_2$-TPR) measurements were carried out with a H$_2$/N$_2$ mixture (10 mol.% H$_2$) and flow rate 50 ml min^{-1}. Linear increase of temperature was 20 °C min^{-1} up to 900 °C. Changes in H$_2$ concentration were detected using a thermal conductivity detector. In order to calculate absolute values of the hydrogen consumed during the samples' reduction, reduction of the grained CuO (0.160–0.315 mm) was performed.

4.3. Catalytic Tests

The catalytic activities of the prepared catalysts were examined in the model reaction, total oxidation of ethanol [20]. Eight sieves were placed into the thin stainless-steel cylinder (diameter 25 mm) to simulate monolithic catalysts. Reaction temperature was increased from 100 to 400 °C with a temperature ramp of 2 °C min^{-1}. Inlet ethanol concentration in the air was 760 ± 10 ppm and space velocity F/W= 21 ± 1 L h g^{-1}. Reaction products were analyzed using a Hewlett–Packard 6890 gas chromatograph (Santa Clara, CA, U.S.A.) equipped with a FID detector and a capillary column (HP–5 19,091 J–413, 30 m × 0.32 mm × 0.25 mm with 5% phenyl methyl silicone). As measures of the catalysts performance temperatures T_{50} and $T_{95}CO_2$ (the temperatures, at which 50% of ethanol conversion and 95% conversion of organic compounds to CO_2 were achieved) were chosen. Ethanol conversions at 200 °C and corresponding reaction rates per gram of active components were determined as well. Selectivity of the catalysts with respect to acetaldehyde and carbon monoxide was characterized as maximum concentrations of acetaldehyde and carbon monoxide and by temperatures, at which they were observed.

5. Conclusions

The experimental study has shown that RF magnetron sputtering of cobalt followed by calcination in air is a promising tool for the deposition of cobalt oxide thin films on stainless-steel meshes. The catalysts prepared by magnetron sputtering in inert atmosphere exhibited relatively low activity in deep oxidation of ethanol. The catalysts efficiency was considerably improved when cobalt was sputtered in oxidation (Ar+O_2) atmosphere and direct oxidation of cobalt particles occurred during the deposition on the support. These catalysts exhibited higher catalytic performance than the pelletized commercial Co_3O_4 catalyst with 50 times higher content of cobalt oxide. Moreover, the sputtered catalysts showed much better adhesion of the Co_3O_4 coating to the support than the catalyst prepared by impregnation with aqueous solution of cobalt nitrate and subsequent heating. Comparison of specific activities revealed the size of cobalt oxide particles as an important parameter for oxidation activity: Smaller particle size led to increased catalytic activity. Finally, the sputtered catalysts showed much better adhesion of the Co_3O_4 coating to the support than the catalyst prepared by impregnation with aqueous solution of cobalt nitrate and subsequent heating.

Supplementary Materials: The following are available online at http://www.mdpi.com/2073-4344/9/10/806/s1, Figure S1: SEM images documenting surface morphology of the prepared catalysts: a) Co-RF-1, b) Co-RF-2, c) Co-RF-3, d) Co-RF-ox/ap, e) Co-RF-ox, f) Co-I, and g) pelletized commercial Co_3O_4 (PEL)

References

1. Duprez, D.; Cavani, F. *Handbook of Advanced Methods and Processes in Oxidation Catalysis*; Imperial College Press: London, UK, 2014.
2. Ojala, S.; Pitkaaho, S.; Laitinen, T.; Koivikko, N.N.; Brahmi, R.; Gaálová, J.; Matějová, L.; Kucherov, A.; Paivarinta, S.; Hirschmann, C.; et al. Catalysis in VOC abatement. *Top. Catal.* **2011**, *54*, 1224–1256. [CrossRef]
3. Jirátová, K.; Kovanda, F.; Balabánová, J.; Kšírová, P. Aluminum wire meshes coated with Co-Mn-Al and Co oxides as catalysts for deep ethanol oxidation. *Catal. Today* **2018**, *304*, 165–171. [CrossRef]

4. Solsona, B.; Davies, T.E.; García, T.; Vázquez, I.; Dejoza, A.; Taylor, S.H. Total oxidation of propane using nanocrystalline cobalt oxide and supported cobalt oxide catalysts. *Appl. Catal. B Environ.* **2008**, *84*, 176–184. [CrossRef]

5. Garcia, T.; Agouram, S.; Sanchez-Royo, J.F.; Murillo, R.; Maria Mastral, A.; Aranda, A.; Vazquez, I.; Dejoz, A.; Solsona, B. Deep oxidation of volatile organic compounds using ordered cobalt oxides prepared by a nanocasting route. *Appl. Catal. A* **2010**, *386*, 16–27. [CrossRef]

6. Liu, Q.; Wang, L.C.; Chen, M.; Cao, Y.; He, H.Y.; Fan, K.N. Dry citrate-precursor synthesized nanocrystalline cobalt oxide as highly active catalyst for total oxidation of propane. *J. Catal.* **2009**, *263*, 104–113. [CrossRef]

7. Xie, S.; Deng, J.; Zang, S.; Yang, H.; Guo, G.; Arandiyan, H.; Dai, H. Au–Pd/3DOM Co_3O_4: Highly active and stable nanocatalysts for toluene oxidation. *J. Catal.* **2015**, *322*, 38–48. [CrossRef]

8. Yang, H.; Dai, H.; Deng, J.; Xie, S.; Han, W.; Tan, W.; Jiang, Y.; Au, C. Porous Cube-Aggregated Co_3O_4 Microsphere-Supported Gold Nanoparticles for Oxidation of Carbon Monoxide and Toluene. *ChemSusChem* **2014**, *7*, 1745–1754. [CrossRef] [PubMed]

9. Bai, B.; Arandiyan, H.; Li, J. Comparison of the performance for oxidation of formaldehyde on nano- Co3O4, 2D-Co_3O_4, and 3D-Co_3O_4 catalysts. *Appl. Catal. B* **2013**, *142*, 677–683. [CrossRef]

10. Kovanda, F.; Jirátová, K.; Ludvíková, J.; Raabová, H. Co–Mn–Al mixed oxides on anodized aluminum supports and their use as catalysts in the total oxidation of ethanol. *Appl. Catal. A* **2013**, *464–465*, 181–190. [CrossRef]

11. Twigg, M.V.; Webster, D.E. *Structured Catalysts and Reactors*, 2nd ed.; Cybulski, A., Moulijn, J.A., Eds.; Chemical Industries Series; Taylor and Francis: Abingdon-on-Thames, UK, 2006; Volume 110, p. 71.

12. Sanz, O.; Banus, E.D.; Goya, A.; Larumbe, H.; Delgado, J.J.; Monzón, A.; Montes, M. Stacked wire-mesh monoliths for VOCs combustion: Effect of the mesh-opening in the catalytic performance. *Catal. Today* **2017**, *296*, 76–83. [CrossRef]

13. Guo, H.; Xue, B.; Chen, M. Catalytic oxidation of VOCs over the structured bimetallic catalyst 0.1% Pt-0.75% CeO_2/SSWM. *Sustain. Environ. Res.* **2015**, *25*, 167–170.

14. Ahlstroem-Silverstand, A.F.; Odenbrand, C.U.I. Modelling catalytic combustion of carbon monoxide and hydrocarbons over catalytically active wire meshes. *Chem. Eng. J.* **1999**, *73*, 205–216. [CrossRef]

15. Klyushina, A.; Pacultová, K.; Krejčová, S.; Słowik, G.; Jirátová, K.; Kovanda, F.; Ryczkowski, J.; Obalová, L. Advantages of stainless steel sieves as support for catalytic N_2O decomposition over K-doped Co_3O_4. *Catal. Today* **2015**, *257*, 2–10. [CrossRef]

16. del Río, L.; López, I.; Marbán, G. Stainless steel wire mesh-supported Co_3O_4 catalysts in the steam reforming of ethanol. *Appl. Catal. B* **2014**, *150–151*, 370–379. [CrossRef]

17. Kouotou, P.M.; Pan, G.F.; Weng, J.J.; Fan, S.B.; Tian, Z.Y. Stainless steel grid mesh-supported CVD made Co_3O_4 thin films for catalytic oxidation of VOCs of olefins type at low temperature. *J. Ind. Eng. Chem.* **2016**, *35*, 253–261. [CrossRef]

18. Ahlstroem-Silverstand, A.F.; Odenbrand, C.U.I. Thermally sprayed wire-mesh catalysts for the purification of flue gases from small-scale combustion of bio-fuel: Catalyst preparation and activity studies. *Appl. Catal. A* **1997**, *153*, 177–201. [CrossRef]

19. Li, Y.; Qui, W.; Qin, F.; Fang, H.; Hadjiev, V.G.; Litvinov, D.; Bao, J. Identification of Cobalt Oxides with Raman Scattering and Fourier Transform Infrared Spectroscopy. *J. Phys. Chem. C* **2016**, *120*, 4511–4516. [CrossRef]

20. Dvořáková, M.; Perekrestov, R.; Kšírová, P.; Balabánová, J.; Jirátová, K.; Maixner, J.; Topka, P.; Rathouský, J.; Koštejn, M.; Čada, M.; et al. Preparation of cobalt oxide catalysts on stainless steel wire mesh by combination of magnetron sputtering and electrochemical deposition. *Catal. Today* **2019**, *334*, 13–23. [CrossRef]

21. Perekrestov, R.; Spesyvyi, A.; Maixner, J.; Mašek, K.; Leiko, O.; Khalakhan, I.; Maňák, J.; Kšírová, P.; Hubička, Z.; Čada, M. The comparative study of electrical, optical and catalytic properties of Co_3O_4 thin nanocrystalline films prepared by reactive high-power impulse and radio frequency magnetron sputtering. *Thin Solid Films* **2019**, *686*, 137–427. [CrossRef]

22. Hadjiev, V.G.; Iliev, M.N.; Vergilov, I.V. The Raman spectra of Co_3O_4. *J. Phys. Chem. Solid State Phys.* **1988**, *21*, 199–201. [CrossRef]

23. Ning, Z.; Jinwen, S.; Mao, S.S.; Liejin, G. Co_3O_4 quantum dots: Reverse micelle synthesis and visible-light-driven photocatalytic overall water splitting. *Chem. Commun.* **2014**, *50*, 2002–2004. [CrossRef]

24. Tang, C.W.; Wang, C.B.; Chen, S.H. Characterization of cobalt oxides studied by FT-IR, Raman, TPR and TG-MS. *Thermochim. Acta* **2008**, *473*, 68–73. [CrossRef]

25. Lenglet, M.; Lopitaux, J.; Terrier, L.; Chartier, P.; Koenig, J.F.; Nkeng, P.; Poillerat, G. Initial Stages of Cobalt Oxidation by FTIR Spectroscopy. *J. Phys. IV* **1993**, *3*, 477–483. [CrossRef]

26. Ghorbani-Moghadam, T.; Kompany, A.; Bagheri-Mohagheghi, M.M.; Abrishami, M.E. Cobalt spin states investigation of Ruddlesden-Popper $La_{2-x}Sr_xCoO_4$, using X-ray diffraction and infrared spectroscopy. *J. Magn. Magn. Mater.* **2018**, *465*, 768–774. [CrossRef]

27. Sexton, B.A.; Hughes, A.E.; Turney, T.W. An XPS and TPR study of the reduction of promoted cobalt-kieselguhr Fischer-Tropsch catalysts. *J. Catal.* **1986**, *97*, 390–406. [CrossRef]

28. Lin, Y.; Chen, Y.W. The mechanism of reduction of cobalt by hydrogen. *Mater. Chem. Phys.* **2004**, *85*, 171–175. [CrossRef]

29. Arnoldy, P.; Moulijn, J.A. Temperature-programmed reduction of CoO/Al_2O_3 catalysts. *J. Catal.* **1985**, *93*, 38–54. [CrossRef]

30. Jirátová, K.; Mikulová, J.; Klempa, J.; Grygar, T.; Bastl, Z.; Kovanda, F. Modification of Co–Mn–Al mixed oxide with potassium and its effect on deep oxidation of VOC. *Appl. Catal. A* **2009**, *361*, 106–116. [CrossRef]

31. Biesinger, M.C.; Payne, B.P.; Grossvenor, A.O.; Lau, L.W.M.; Gerson, A.R. Resolving surface chemical states in XPS analysis of first row transition metals, oxides and hydroxides: Cr, Mn, Fe, Co and Ni. *Appl. Surf. Sci.* **2011**, *257*, 2717–2730. [CrossRef]

32. Davies, T.E.; Garcia, T.; Solsona, B.; Taylor, S.H. Nanocrystalline cobalt oxide: A catalyst for selective alkane oxidation under ambient conditions. *Chem. Commun.* **2006**, *32*, 3417–3419. [CrossRef]

33. Finocchio, E.; Willey, R.J.; Busca, G.; Lorenzelli, V. FTIR studies on the selective oxidation and combustion of light hydrocarbons at metal oxide surfaces. Part 3. Comparison of the oxidation of C3 organic compounds over Co_3O_4, $MgCr_2O_4$ and CuO. *J. Chem. Soc. Faraday Trans.* **1997**, *93*, 175–180. [CrossRef]

34. Šolcová, O.; Matějová, L.; Topka, P.; Musilová, Z.; Schneider, P. Comparison of textural information from argon (87 K) and nitrogen (77 K) physisorption. *J. Porous Mater.* **2011**, *18*, 557–565. [CrossRef]

35. Topka, P.; Jirátová, K.; Soukup, K.; Goliáš, J. Device for Measuring Specific Surface of Large Samples, Method of Measurement and Its Use. Patent Application PV 2019-380; Ústav Chemických Procesů, Prague, Czech Republic, 2019.